Biophysical Chemistry 167 (2012) 1–7

Contents lists available at SciVerse ScienceDirect

Biophysical Chemistry

journal homepage: http://www.elsevier.com/locate/biophyschem

Conformational dynamics of human IAPP monomers

Ronan D. Murphy [a,b], Jennifer Conlon [a], Tayyaub Mansoor [a], Sorin Luca [c], Sara M. Vaiana [d,e], Nicolae-Viorel Buchete [a,b,*]

[a] School of Physics, University College Dublin, Belfield, Dublin 4, Ireland
[b] Complex and Adaptive Systems Laboratory, University College Dublin, Belfield, Dublin 4, Ireland
[c] Department of Pharmaceutical Sciences, University of Nebraska, Omaha, NE 68198, USA
[d] Center for Biological Physics, Arizona State University, Tempe, AZ 85287, USA
[e] Department of Physics, Arizona State University, Tempe, AZ 85287, USA

HIGHLIGHTS

► Kinetic clustering of conformational states of human IAPP monomers.
► Partially structured hIAPP conformational states correspond to several end-to-end distances.
► Conformational dynamics of hIAPP monomers and dimers driven by hydrophobic packing.
► PCA as an unbiased, data-driven approach to identify conformational states.

GRAPHICAL ABSTRACT

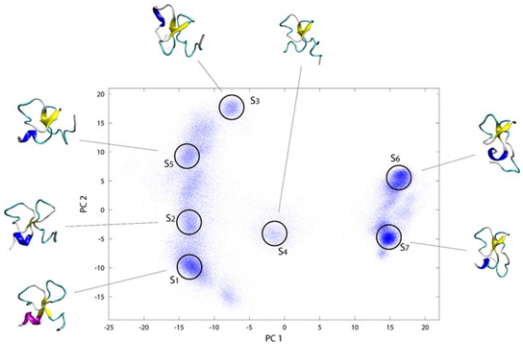

ARTICLE INFO

Article history:
Received 26 January 2012
Received in revised form 23 March 2012
Accepted 25 March 2012
Available online 5 April 2012

Keywords:
Human Islet Amyloid Polypeptide (hIAPP)
Molecular dynamics
Type 2 diabetes
Conformational analysis
Data-driven kinetic analysis

ABSTRACT

We study the conformational dynamics of the human Islet Amyloid Polypeptide (hIAPP) molecule – a 37 residue-long peptide associated to type 2 diabetes – using molecular dynamics (MD) simulations. We identify partially structured conformational states of the hIAPP monomer, categorized by both end-to-end distance and secondary structure, as suggested by previous experimental and computational studies. The MD trajectories of hIAPP are analyzed using data-driven methods, in particular principal component analysis, in order to identify preferred conformational states of the amylin monomer and to discuss their relative stability as compared to corresponding states in the amylin dimer. These potential hIAPP conformational states could be further tested and described experimentally, or in conjunction with modern computational analysis tools such as Markov state-based methods for extracting kinetics and thermodynamics from atomistic MD trajectories.

1. Introduction

Human Islet Amyloid Polypeptide (hIAPP) or Amylin is a naturally occurring 37 residue-long peptide that is co-secreted with insulin by the β-cells of the pancreas and also, in small amounts, by other organs [1]. The hIAPP molecule is commonly found in patients suffering with type 2 diabetes where it presents itself in fibril form (Fig. 1a) [2]. As a result, understanding the oligomerization and fibril formation molecular mechanisms of hIAPP [2–6] is a central topic of current diabetes-related research.

Recently, solid state nuclear magnetic resonance studies (ssNMR) have revealed for the first time atomically detailed models of the

* Corresponding author at: School of Physics, University College Dublin, Belfield, Dublin 4, Ireland.
E-mail address: buchete@ucd.ie (N.-V. Buchete).

0301-4622/$ – see front matter © 2012 Elsevier B.V. All rights reserved.
doi:10.1016/j.bpc.2012.03.010

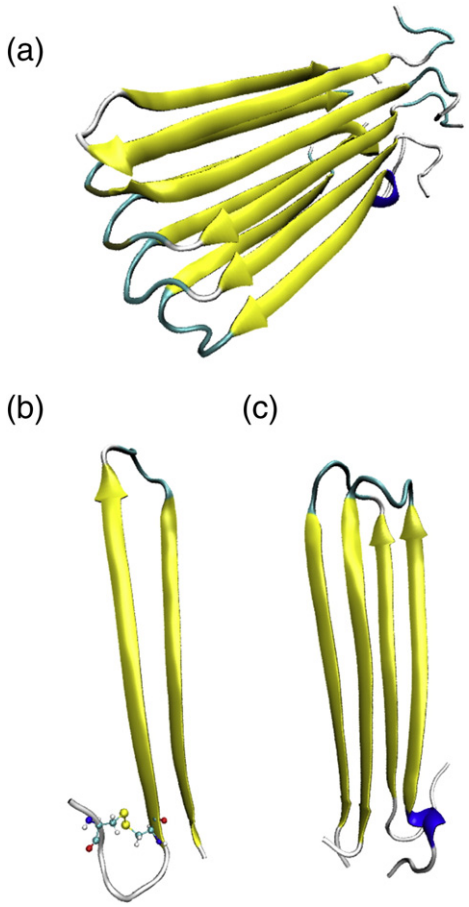

Fig. 1. Molecular model of the hIAPP fibril structure (a) from Ref. [2], and fibril-compatible hIAPP monomer (b), and dimer (c) structures, selected from the fibril fragment shown in (a).

molecular structure of protofilaments formed by hIAPP [2]. Subsequently, several studies have been performed to model fibrils and oligomers of both hIAPP and the rat variant rIAPP [7–11]. However, mainly due to its rich conformational dynamics, the structural states of the amylin monomer (a fibril-compatible one is shown in Fig. 1b), and in particular its kinetic behavior during the early processes of oligomerization and fibril formation, are less well known.

The conformational dynamics of the hIAPP monomer has been studied recently both experimentally and computationally [4–6,12–14]. In particular, the recent study of Vaiana et al. [5] examined both the hIAPP and rIAPP monomers in terms of the observed end-to-end distances, between the N terminal CYS2-CYS7 disulfide bond and the C-terminal tryptophan (which was mutated from the wild type tyrosine), both experimentally, by using an innovative tryptophan triplet quenching (TTQ) technique, and computationally, by using carefully designed molecular dynamics (MD) simulations with explicit solvent. That study provided strong evidence that the preferential conformational states of hIAPP and rIAPP monomers may differ significantly [5].

Though novel experimental techniques, such as the studies mentioned above [2,5,6], allow extracting unprecedented information on the conformational dynamics of peptides and proteins such as IAPP that lack a well-defined 3-dimensional structure, these techniques convey only partial information on their intrinsic conformational dynamics. This is due to data being observed only along specific reaction coordinates (e.g., end-to-end distance from TTQ and FRET or secondary structure elements from NMR measurements). It thus appears to be a gap in our understanding of the relation between global large scale motions (as detected by end-to-end distance methods) and the specific local changes in secondary structure and local contacts (as detected by NMR). In principle, MD simulations offer a means to bridge this gap, though the statistical analysis of the large amounts of data provided remains a challenge. Recent advances in kinetic analysis and rate extraction methods from MD simulations, coupled to enhanced sampling approaches [15–17], could provide a way to access and analyze both global (i.e., as reflected by collective variables) and local (i.e., backbone dihedral angles and local contacts) structural information.

Here, we perform extensive molecular dynamics (MD) simulations of hIAPP molecules, treated both as water solvated monomers, and also as part of their molecular homo-dimers, to investigate the intrinsic conformational dynamics of these peptides, and to characterize in detail the partially structured conformations sampled in the simulation trajectories. In our analysis, we use both the end-to-end distance (i.e., the distance between the N and C-terminal side chains, LYS1 and TYR37), as needed for comparison to previous experimental and computational studies, as well as less biased, data-driven methods based on principal component analysis (PCA), to cluster the conformational states generated by our simulations and to extract and analyze the corresponding representative structures.

Interestingly, beyond its relevance to understanding the conformational dynamics of hIAPP molecules, the results of this study suggest a new approach for developing methods that could provide an initially unbiased identification of putative conformational states of peptides and proteins observed in simulation trajectories. These states could be further tested and described by using other modern trajectory analysis approaches such as Markov state-based methods for extracting kinetics and thermodynamics from molecular simulations [16–20]. The generality of these methods makes them applicable to both coarse-grained [21–24], and to atomistic molecular modeling studies of peptides, proteins or enzymes [16,25–28], where specific conformational changes need to be identified.

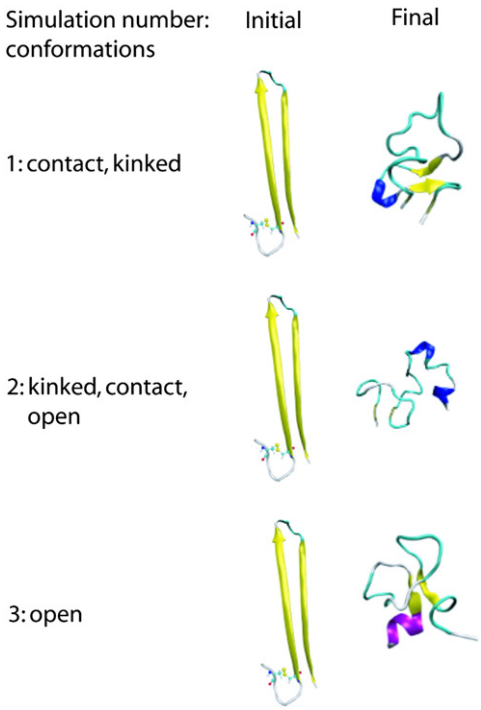

Fig. 2. Initial and final structures of the first set of simulations initialized from fibril-compatible monomer structures, and the corresponding conformations sampled based on end-to-end distance values [5]. All three simulations were run for 50 ns.

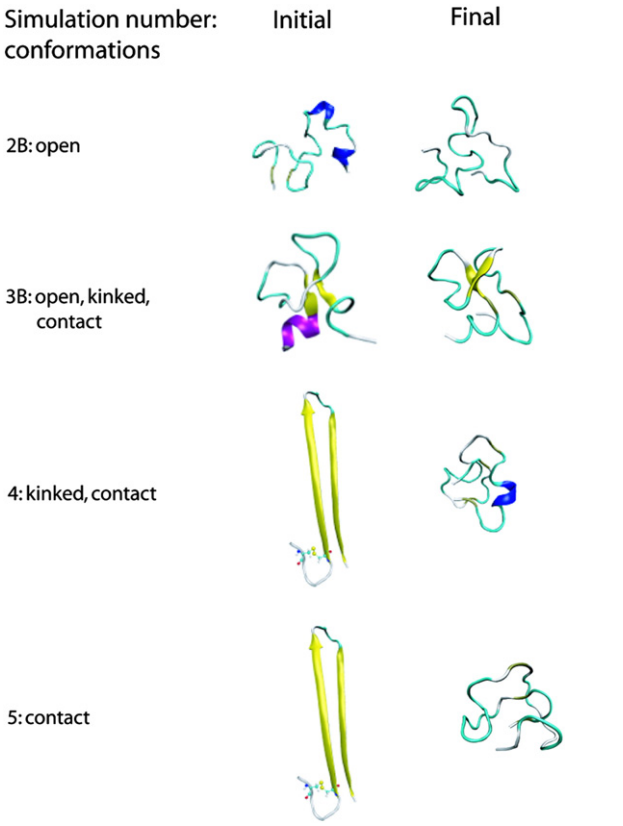

Fig. 3. The corresponding conformations sampled [5], and the initial and final structures of the second set of 100 ns-long monomer simulations that were initiated from both partially structured and fibril-like initial conformations.

2. Methods

We use the molecular dynamics package GROMACS 4.5.3 [29] to perform MD simulations of the amylin monomer in implicit solvent. The monomer structures were taken from the fibril structure reported by Luca et al. [2], because, to date, they are most supported by both experimental and modeling studies [2]. At the same time, for monomers and dimers, the fibril-like structures, while accessible, they are known to be of significantly high free energy, and could lead thus to rapid sampling of other, alternative structures. The CYS2-CYS7 disulfide bond was kept intact, as shown in Fig. 1b. To achieve enhanced conformational sampling in near-physiological conditions, we adopted the generalized Born implicit solvent model, GBSA [30–32], and used infinite cut-offs for all long-range interactions since implicit solvent simulations do not require periodic boundary conditions. The GBSA implicit solvent model has been extensively used in peptide and nucleic acid simulations [30–35]. Though we note that a loss of accuracy may be expected when compared to the use of explicit (i.e., all-atom) water models, using GBSA is well justified in proof of concept studies, such as ours, where the analysis methods and the discussion (e.g., the possibility to identify the existence of several conformational states for certain d_{EE} values) do not require very accurate calculations of solvation energies. The surface tension was set to 2.05016 kJ/mol/nm^2, the default value for the model used, which is recommended in the absence of additional *a priori* information. A time-step of 2 fs was used, and all simulations were performed at an absolute temperature of 300 K. The Amber99SB [36] force-field was used to model the proteins, as it was shown to provide a good balance for the formation of the different secondary structure elements in the case of small peptides [37]. The analysis performed consisted of end-to-end distance, solvent-accessible-surface-area, and secondary-structure calculations, as well as principal component analysis. The total simulation time for the monomers was 550 ns, as detailed in Figs. 2 and 3, with a further 150 ns (i.e., three simulations of 50 ns each) of MD simulations performed for the case of amylin dimers (initial structure illustrated in Fig. 1c), for comparison. Note that all our initial runs were started from experimentally derived fibril-compatible conformations, except the cases 2B and 3B indicated in Fig. 3, which were initiated based on runs 2 and 3 shown in Fig. 2. To illustrate convergence, a comparison of end-to-end distance distributions for full simulation time versus half simulation time is made in the supplementary data (Figure S1).

3. Results and Discussion

An overview of our monomer simulations is presented in Figs. 2 and 3, with the corresponding behavior of the end-to-end distance (d_{EE}) over the course of each simulation indicated in the last column.

As shown, the first monomer simulations were initiated from the representative fibril-compatible conformations (Fig. 1b). In all cases, we observed a fast initial hydrophobic collapse of the initial experimentally tested 'fibril-like' conformation to structures corresponding to the contact ($d_{EE} \approx 5$ Å), 'kinked' ($d_{EE} \approx 5$ to 11 Å) or 'open' ($d_{EE} > 11$ Å) end-to-end distance values, as defined in Ref. [5].

The final structures of simulations 2 and 3 were used subsequently as starting structures for two additional 100 ns simulations (labeled 2B and 3B in Fig. 3), in an effort to observe further open-contact transitions. In agreement with Ref. [5], we see no definite relation between secondary structure content and end-to-end distance conformations in the simulations presented for the kinked states. We also observed the same behavior for the open and contact states as well. For example, in simulations 1, 3B, 4 and 5, we identify contact structures, with end-to-end distances at around 5 Å maintained throughout the majority of each simulation (Figs. 2 and 3), and we see both β-sheet and helical structures occurring with high frequency in simulations 1 and 3B, while trajectories 4 and 5 are characterized by mostly random coil structures. Simulations 2 and 3 contain predominantly open structures, though the actual ensemble of molecular structures sampled is very diverse. While we, therefore, cannot identify well-defined conformations characterized only based on end-to-end distances, we do see some interesting structural transitions between the d_{EE}-based conformational basins in some of the simulations, as illustrated in Figs. 2–4.

3.1. End-to-end distance analysis

Molecular structural analysis such as end-to-end distance calculations were performed using VMD [38]. The first three 50 ns simulations show different end-to-end distance behaviour. The first simulation, illustrated in Fig. 4a, shows a stable 'contact' conformation, with brief transitions to 'kinked' conformations. The second simulation shows a stable 'open' conformation, as it was also observed in simulation 3. Note that the similarities in the end-to-end distance values for simulations 2 and 3 could be misleading, because looking at the actual structures in the simulations indicates that the 'open' conformation could correspond to an ensemble with a wide range of underlying structures. This would be expected since the open state is likely entropy-driven. To investigate these differences even further, two more simulations were run, this time from the end structures of simulations 2 and 3, for 100 ns each, labelled 2B and 3B for clarity. The hIAPP end-to-end distance in simulation 2B does not vary significantly but, nevertheless, transitions between end-to-end regions are observed in trajectory 3B, as illustrated in Fig. 5b.

Due to all three end-to-end conformations being sampled in simulation 3B, we pay particular attention to it. Fig. 5a illustrates the secondary-structure evolution over time for the simulation,

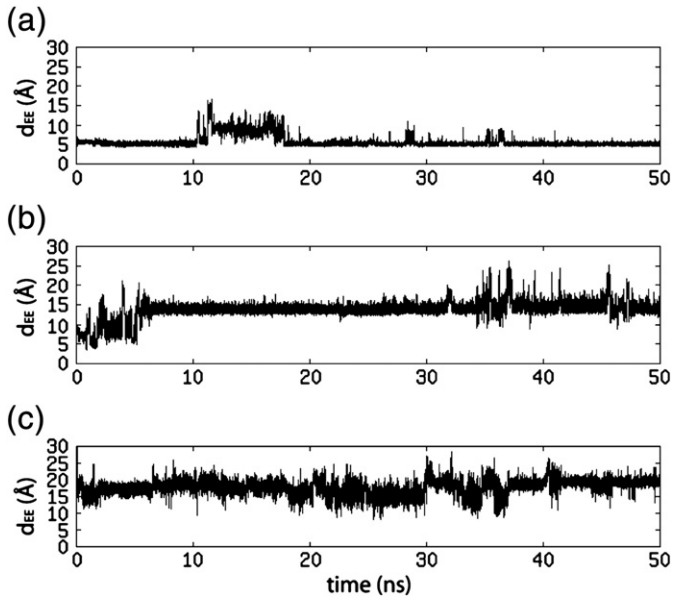

Fig. 4. End-to-end distances calculated for the first three simulations listed in Fig. 2.

computed using the STRIDE [39] plug-in in VMD [38]. In particular, between 25 and 35 ns we see a reordering of the beta-sheet regions prior to the 'open'–'closed' transition. This is a possible indication that a secondary-structure rearrangement facilitates the transition, at least in this case. Fig. 3 shows the starting and final structures. We use the term 'spine' to describe the region of the hIAPP monomer conformation where the beta-sheet was located at the beginning of the simulation. The beta-sheet was originally located along the backbone 'spine' of the conformation but is shifted to a beta-sheet linking of one side of the spine to the loop connecting the two parts of the residual 'spine' structure. Although the C-terminal helix is preserved, the secondary-structure algorithm does not formally identify it as being present in the final structure, but is identified only transiently throughout the simulation time, as depicted in Fig. 5a.

3.2. Solvent accessible surface area calculations

Another measure that is relevant to the intrinsic conformational dynamics of hIAPP monomers is the solvent-accessible-surface-area (SASA). The hydrophobic SASA fraction, corresponding to the hydrophobic residues of the amylin peptide, gives good insight into the stability of these structures in an aqueous environment. The SASA calculations were performed using analysis tools from the GROMACS package [29]. The observed immediate 'collapse' of the initial (i.e., 'fibril-like') structure can be attributed largely to a typical hydrophobic collapse mechanism, seen in the rapid decrease of SASA values for both hydrophobic and non-hydrophobic residues. All three of the initial 50 ns simulations show this behaviour for both hydrophobic and hydrophilic residues. The hydrophobic SASA of the initial fibril-compatible structure is 12.2 nm^2, larger than the values of the collapsed conformations, as seen in the distributions illustrated in Fig. 6. Subsequent conformational shifts do not display a pronounced change in the hydrophobic SASA fraction, however. Comparisons are made here with three 50 ns simulations of the corresponding hIAPP monomers from an amylin dimer, using the same simulation conditions and parameters in order to facilitate a direct SASA comparison. In each of these simulations, the dimers maintained their overall structure, not dissociating or undergoing extensive hydrophobic collapse. As illustrated in Fig. 6, we find that the collapsed monomer structures have a larger hydrophobic SASA area than either of the chains of the dimer, indicating that burial of hydrophobic residues contributes indeed to stabilizing the dimer conformations in solution. We note, however, that further more extensive studies should lead to properly converged, 'putative' IAPP dimmers, which are likely to have significantly different structures than the ones obtained here starting from fibril-like conformations. Nevertheless, our simple tests allow the semi-quantitative description of the early conformational changes that could occur along fibril association-dissociation pathways for hIAPP monomers and dimers.

3.3. Principal component analysis

The choice of optimal reaction coordinates for the analysis of molecular dynamics simulations of biomolecules is notoriously a difficult one. The choice is often motivated by simplicity, such as for RMSD, or to facilitate comparison with experimental observables, such as the end-to-end distance in tryptophan triplet quenching experiments [5]. However, besides the advantage of using an observable that captures global, collective aspects of conformational changes, there are also evident disadvantages associated with choosing a predefined reaction coordinate, or set of reaction coordinates. The main problem is that there is often a subjective bias being introduced into the analysis as a result of the low-dimensional projection of higher-dimensional free energy landscapes [40]. A preferable method for reducing the complexity of simulation data while still capturing the intrinsic conformational dynamics could be to use reaction coordinates that are data-driven rather than purely geometrical or convention-driven.

Here, we show results obtained by principal component analysis (PCA) of simulation 3B, discussed in detail above. PCA is used to reduce the complex motions of the original MD data into collective motions along a set of orthogonal components, with the first component describing the largest of these collective motions. What we lose in this process is an analytical expression that describes our reaction coordinate, although observation of the individual components superimposed onto the simulation trajectory allows us to identify the motions involved. We also note that the motions corresponding to each component will differ for each simulation, due to the data-driven nature of the analysis. The PCA in this study was done using the WORDOM analysis package [41]. In this work, to illustrate the concept clearly, we are only interested in the first two main modes of the PCA (i.e., the two components accounting for the largest collective motions of the data), and we use them to cluster conformations into 'conformational states'. This particular method suggests the feasibility of a more general, and possibly automatic, classification of states that is data-driven, and therefore applicable to virtually any system under study. Subsequently, the discrete inter-state dynamics could be analysed using a Markovian approach [16–20, 42]. We note that, while PCA has been used in molecular dynamics studies of other proteins in the past [43,44], here we find it useful in the context of identifying conformational basins of hIAPP beyond the simple d_{EE}-based conformational clustering. Recent studies have also proposed improvements in the PCA method, such as using PCA by parts [43], and new data-driven methods have been developed such as non-metric multidimensional scaling (nMDS) [45]. Our present study is limited to a proof-of-principle comparison of 'conventional' PCA data-driven methods with more typically encountered *ad hoc* defined (and often one-dimensional) reaction coordinates, and we note appeal of using PCA further in potentially less biased kinetic analysis methods.

The PCA data is analysed and presented here in two forms. In Fig. 7, the time-series of the first two modes is shown. Note the slight decrease in variance in the second mode, PC2 (-17 to $+20$) relative to the first mode, PC1 (-25 to $+20$), as would be expected. In Fig. 8, a scatter plot of the same two modes is shown. The seven clusters illustrated in Fig. 8, labelled S_1 to S_7, were identified using only these first two PCA components, and correspond directly to the regions highlighted in green in Fig. 7. Representative structural conformations corresponding to each cluster are also shown, and labelled according to the order in which

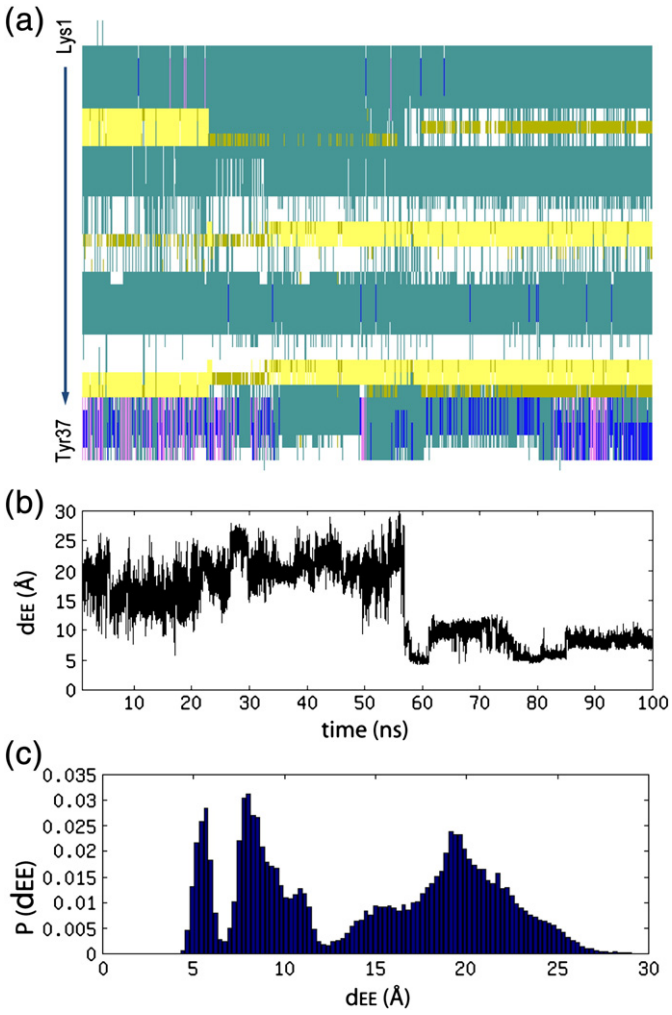

Fig. 5. Time evolution of (a) the secondary structure content, and (b) the end-to-end distance calculated for the simulation 3B listed in Fig. 3 (c) Probability distribution of the end-to-end distance for simulation 3B. In (a) the y-axis represents the hIAPP sequence, with LYS1 at the top and TYR37 at the bottom. The x-axis is the same as in (b). Yellow corresponds to beta-sheet, pink-blue corresponds to helix, and white/green corresponds to coil.

they are visited along the trajectory. We note that here we use simulation 3B, due to its better sampling of all three end-to-end distance states, and to the large beta-sheet content, which makes the sampled structures good candidates for aggregation-prone conformations. However, we have also used PCA on multiple trajectories, and a discussion is provided in the supplementary data (Figure S2).

The first principal component, PC1, does indeed appear to capture quite well the end-to-end distance transition discussed earlier and illustrated in Fig. 5b. This is an additional indication that d_{EE}-based TTQ or FRET experiments could be particularly useful in capturing essential features of the intrinsic hIAPP dynamics.

In Fig. 5a, the loss of the original beta-strand from the 'spine' of the monomer is observed at just over 20 ns into the MD simulation. Note that this was not reflected in the end-to-end distance calculation shown in Fig. 5a. However, in Fig. 8 we see a clear evidence of a change in structure, corresponding to the S_2 cluster. The representative conformation corresponding to this S_2 cluster is also shown in Fig. 8, with the beta-sheet no longer present.

While the clusters presented here were identified based simply on the evident probability density differences illustrated in Fig. 8, an automatic clustering algorithm such as the K-means or the Jarvis-Patrick method [46] could also be used. Coupled with a data-driven approach such as PCA, an effective automatic clustering method should facilitate future studies that would allow us to run a simulation, project the data onto the main principal components, and cluster the resulting data into individual conformational basins, all in one step. Furthermore, if we coupled the resulting assignment with a Markov state-based kinetic analysis, we could feasibly go from starting a typical MD simulation to obtaining the desired kinetic and thermodynamic information without any further user input requested. This approach would be similar in its goals, though not necessarily in its implementation with other recently proposed algorithms such as MSMBuilder [19,20], for example. Perhaps the most attractive aspect of an approach of this nature is that it avoids any bias that may be introduced by an often arbitrary selection of geometry-based reaction coordinates. What we appear to lose, is that the motional characteristics identified by our PCA-based analysis are expected to vary with every data-set, and cannot be thus connected *a priori* to representative conformational states. Nevertheless, for kinetic clustering purposes this is actually a desirable trait, since a well-defined geometric metrics will seldom be able to identify effectively variance in a simulation, while the more general PCA data-driven methods are designed to do exactly that.

4. Conclusions

In this work, we use structural information revealed by previous experimental and computational studies to probe and analyze the conformational dynamics of hIAPP molecules. While this study is focused on the dynamics of amylin monomers in water, under dilute conditions, several simulations of dimers (initialized from fibril-like conformations) were also performed, in order to assess the main conformational differences that may occur early along the amylin fibril dissociation/aggregation pathways.

Our extensive amylin monomer simulations reveal several partially structured conformational states that the hIAPP peptide monomers can adopt, which could correspond to different end-to-end distance values that may be indeed occurring experimentally [5]. Moreover, we observe and describe transitions occurring between the 'open', 'kinked' and 'contact'-type conformations reported earlier [5]. Our results show that the end-to-end distance, while sometimes useful for describing large-scale conformational changes, is rather poor at identifying differences between specific conformational states, in particular when changes in secondary structure are involved. Nevertheless, in conjunction with extensive molecular simulations, even a relatively ambiguous, global reaction coordinate such as the end-to-end distance

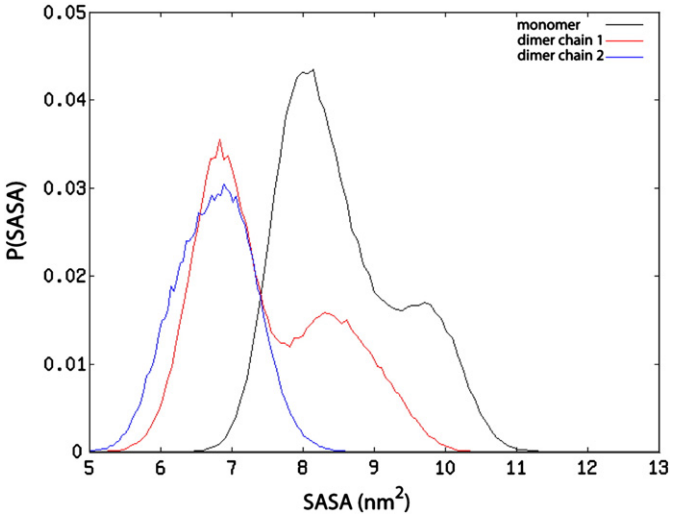

Fig. 6. Hydrophobic solvent accessible surface area (SASA) normalized histograms calculated for the first three monomer simulations in Fig. 2 (black), and for each of the two peptides chains (i.e., chain 1 red, and chain 2 blue) calculated for the three dimer simulations of 50 ns each (see text for details). Note that generally lower hydrophobic SASA values are correlated with higher conformational stabilities in water, as observed for each of the peptide chains that form the amylin dimer.

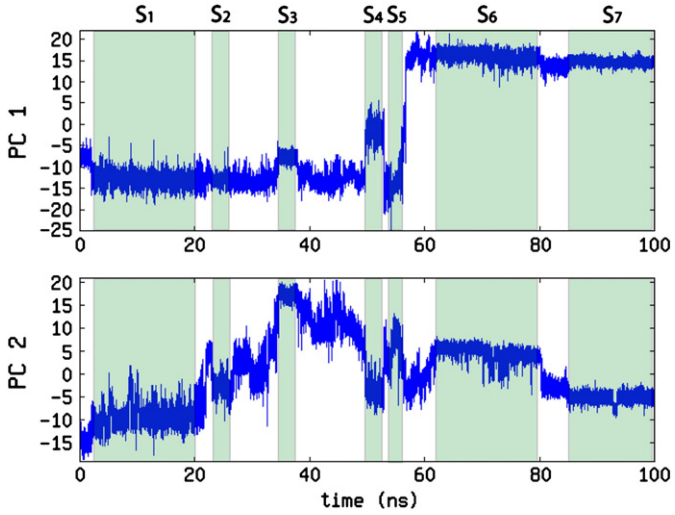

Fig. 7. Time evolution of the two most dominant modes of motion (i.e., principal components PC1 and PC2) calculated by principal component analysis (PCA) for simulation 3B.

can still provide unique insights into the detailed conformational dynamics of intrinsically disordered proteins such hIAPP [5].

In order to provide relevant support for a deeper understanding of experimental results, the statistical analysis of the large amounts of data provided by molecular simulations remains a challenging topic. Our results suggest that significant progress can be achieved by developing and using *data-driven* methods for categorizing conformational change in biomolecules, without biasing the analysis with the use of specific, *a priori* proposed reaction coordinates. Here, we apply such a data-driven approach based on principal component analysis to the semi-automatic categorization of underlying free energy surface of the 37-residue long hIAPP molecule. Our analysis permits the identification of several conformations in which the amylin peptide adopts partially structured states, in agreement with previous experimental and computational studies [5].

Additionally, we compared the hydrophobic fraction of the solvent accessible surface area of hIAPP peptides during their conformational dynamics in a fibril-compatible amylin dimer, to the corresponding SASA values of water solvated monomers. We find that hydrophobic side chain packing is a major driving force responsible for the overall stabilization of the dimer molecular ensemble.

We envision that data-driven methods for analyzing the multi-dimensional conformational space of biomolecules, such as the ones used here for amylin, could be particularly useful for providing an unbiased and possibly automatic, real-time identification and analysis of putative conformational states of peptides and proteins. These states could be further tested and described by using other modern approaches such as Markov state-based analysis for extracting their equilibrium populations and the corresponding transition rates from MD trajectories [16,17]. While there are also several inherent limitations to using a purely PCA-based method due to its linear nature, there are nevertheless other potential approaches based on non-liner formulations of the method that could be applied to larger-scale simulations where larger portions of the underlying energy surface may be mapped and categorized. The simpler approach presented here, appears to be nevertheless a useful tool in categorizing the free energy basins of the hIAPP monomer, avoiding some of the bias and enhancing the interpretation offered by observations along simple, though often experimentally useful, low-dimensional reaction coordinates such as the end-to-end distance.

Acknowledgements

We thank Robert B. Best for helpful discussions and Robert Tycko for kindly providing the coordinates of the molecular models of hIAPP

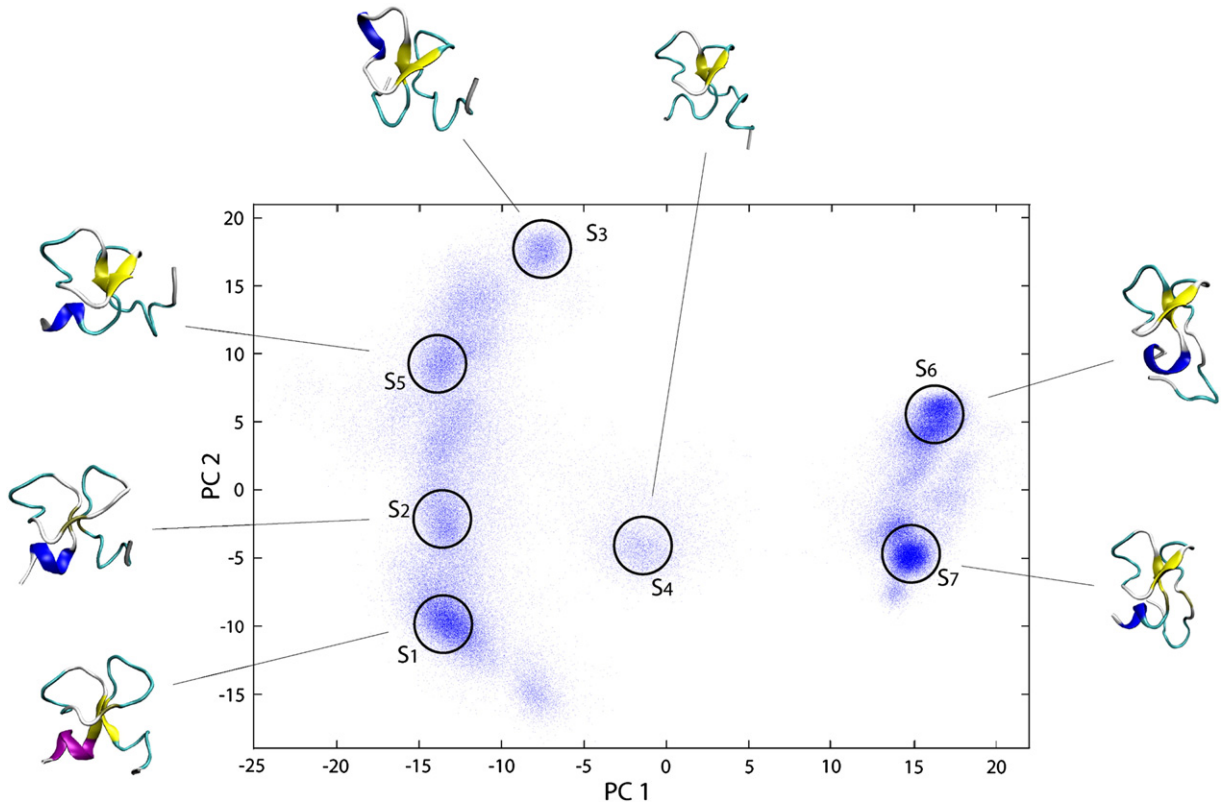

Fig. 8. Cross-correlation of the two dominant modes of motion (i.e., principal components PC1 and PC2) calculated for the data in simulation 3B. Representative molecular conformations of hIAPP molecules corresponding to each of the seven main clusters are shown.

protofilaments. We gratefully acknowledge financial support from the Irish Research Council for Science, Engineering and Technology (IRCSET), and the use of computational facilities provided by the Irish Centre for High-End Computing (ICHEC).

Appendix A. Supplementary data

Supplementary data to this article can be found online at doi:10.1016/j.bpc.2012.03.010.

References

[1] M.R. Hayden, Islet amyloid, metabolic syndrome, and the natural progressive history of type 2 diabetes mellitus, JOP 3 (2002) 126–138.
[2] S. Luca, W.M. Yau, R. Leapman, R. Tycko, Peptide conformation and supramolecular organization in amylin fibrils: Constraints from solid-state NMR, Biochemistry 46 (2007) 13505–13522.
[3] R. Mishra, B. Bulic, D. Sellin, S. Jha, H. Waldmann, R. Winter, Small-molecule inhibitors of islet amyloid polypeptide fibril formation, Angewandte Chemie International Edition 47 (2008) 4679–4682.
[4] R. Mishra, M. Geyer, R. Winter, NMR Spectroscopic Investigation of Early Events in IAPP Amyloid Fibril Formation, ChemBioChem 10 (2009) 1769–1772.
[5] S.M. Vaiana, R.B. Best, W.M. Yau, W.A. Eaton, J. Hofrichter, Evidence for a Partially Structured State of the Amylin Monomer, Biophysical Journal 97 (2009) 2948–2957.
[6] S.M. Vaiana, R. Ghirlando, W.M. Yau, W.A. Eaton, J. Hofrichter, Sedimentation studies on human amylin fail to detect low-molecular-weight oligomers, Biophysical Journal 94 (2008) L45–L47.
[7] K. Weise, D. Radovan, A. Gohlke, N. Opitz, R. Winter, Interaction of hIAPP with Model Raft Membranes and Pancreatic beta-Cells: Cytotoxicity of hIAPP Oligomers, ChemBioChem 11 (2010) 1280–1290.
[8] Y.A. Domanov, P.K.J. Kinnunen, Islet amyloid polypeptide forms rigid lipid-protein amyloid fibrils on supported phospholipid bilayers, Journal of Molecular Biology 376 (2008) 42–54.
[9] J. Green, C. Goldsbury, T. Min, S. Sunderji, P. Frey, J. Kistler, G. Cooper, U. Aebi, Full-length rat amylin forms fibrils following substitution of single residues from human amylin, Journal of Molecular Biology 326 (2003) 1147–1156.
[10] S. Zraika, R.L. Hull, C.B. Verchere, A. Clark, K.J. Potter, P.E. Fraser, D.P. Raleigh, S.E. Kahn, Toxic oligomers and islet beta cell death: guilty by association or convicted by circumstantial evidence? Diabetologia 53 (2010) 1046–1056.
[11] M.N. Andrews, R. Winter, Comparing the structural properties of human and rat islet amyloid polypeptide by MD computer simulations, Biophysical Chemistry 156 (2011) 43–50.
[12] D. Milardi, M. Pappalardo, M. Pannuzzo, D.M. Grasso, C. La Rosa, The role of the Cys2-Cys7 disulfide bridge in the early steps of Islet amyloid polypeptide aggregation: A molecular dynamics study, Chemical Physics Letters 463 (2008) 396–399.
[13] N.F. Dupuis, C. Wu, J.E. Shea, M.T. Bowers, The Amyloid Formation Mechanism in Human IAPP: Dimers Have beta-Strand Monomer-Monomer Interfaces, Journal of the American Chemical Society 133 (2011) 7240–7243.
[14] R. Kayed, J. Bernhagen, N. Greenfield, K. Sweimeh, H. Brunner, W. Voelter, A. Kapurniotu, Conformational transitions of islet amyloid polypeptide (IAPP) in amyloid formation in vitro, Journal of Molecular Biology 287 (1999) 781–796.
[15] N.V. Buchete, G. Hummer, Peptide folding kinetics from replica exchange molecular dynamics, Physical Review E 77 (2008).
[16] N.V. Buchete, G. Hummer, Coarse master equations for peptide folding dynamics, The Journal of Physical Chemistry. B 112 (2008) 6057–6069.
[17] G.S. Buchner, R.D. Murphy, N.V. Buchete, J. Kubelka, Dynamics of protein folding: Probing the kinetic network of folding-unfolding transitions with experiment and theory, Biochimica et Biophysica Acta Proteins and Proteomics 1814 (2011) 1001–1020.
[18] A.M. Berezhkovskii, F. Tofoleanu, N.V. Buchete, Are Peptides Good Two-State Folders? Journal of Chemical Theory and Computation 7 (2011) 2370–2375.
[19] K.A. Beauchamp, G.R. Bowman, T.J. Lane, L. Maibaum, I.S. Haque, V.S. Pande, MSMBuilder2: Modeling Conformational Dynamics on the Picosecond to Millisecond Scale, Journal of Chemical Theory and Computation 7 (2011) 3412–3419.
[20] G.R. Bowman, K.A. Beauchamp, G. Boxer, V.S. Pande, Progress and challenges in the automated construction of Markov state models for full protein systems, Journal of Chemical Physics 131 (2009).
[21] N.V. Buchete, J.E. Straub, D. Thirumalai, Dissecting contact potentials for proteins: Relative contributions of individual amino acids, Proteins 70 (2008) 119–130.
[22] N.V. Buchete, J.E. Straub, D. Thirumalai, Orientation-dependent coarse-grained potentials derived by statistical analysis of molecular structural databases, Polymer 45 (2004) 597–608.
[23] A.E. van Giessen, J.E. Straub, Coarse-Grained Model of Coil-to-Helix Kinetics Demonstrates the Importance of Multiple Nucleation Sites in Helix Folding, Journal of Chemical Theory and Computation 2 (2006) 674–684.
[24] F. Khatib, F. DiMaio, S. Cooper, M. Kazmierczyk, M. Gilski, S. Krzywda, H. Zabranska, I. Pichova, J. Thompson, Z. Popović, M. Jaskolski, D. Baker, Crystal structure of a monomeric retroviral protease solved by protein folding game players, Nature Structural & Molecular Biology 18 (2011) 1175–1177.
[25] A.L. Milac, N.V. Buchete, T.A. Fritz, G. Hummer, L.A. Tabak, Substrate-induced conformational changes and dynamics of UDP-N-acetylgalactosamine: Polypeptide N-acetylgalactosaminyltransferase-2, Journal of Molecular Biology 373 (2007) 439–451.
[26] E. Rosta, M. Nowotny, W. Yang, G. Hummer, Catalytic mechanism of RNA backbone cleavage by ribonuclease H from quantum mechanics/molecular mechanics simulations, Journal of the American Chemical Society 133 (2011) 8934–8941.
[27] K. Lindorff-Larsen, S. Piana, R.O. Dror, D.E. Shaw, How fast-folding proteins fold, Science 334 (2011) 517–520.
[28] F. Tofoleanu, N.-V. Buchete, Molecular Interactions of Alzheimer's Aβ Protofilaments with Lipid Membranes, Journal of Molecular Biology (2012), doi:10.1016/j.jmb.2011.1012.1063.
[29] B. Hess, C. Kutzner, D. van der Spoel, E. Lindahl, GROMACS 4: Algorithms for highly efficient, load-balanced, and scalable molecular simulation, Journal of Chemical Theory and Computation 4 (2008) 435–447.
[30] V. Tsui, D.A. Case, Theory and applications of the generalized Born solvation model in macromolecular simulations, Biopolymers 56 (2000) 275–291.
[31] D. Onufriev, D. Bashford, D.A. Case, Exploring protein native states and large-scale conformational changes with a modified generalized born model, Proteins 55 (2004) 383–394.
[32] E. Kim, S. Jang, Y. Pak, Consistent free energy landscapes and thermodynamic properties of small proteins based on a single all-atom force field employing an implicit solvation, Journal of Chemical Physics 127 (2007).
[33] V.A. Voelz, K.A. Dill, I. Chorny, Peptoid Conformational Free Energy landscapes From Implicit-Solvent Molecular Simulations in AMBER, Biopolymers 96 (2011) 639–650.
[34] A.K. Felts, Y. Harano, E. Gallicchio, R.M. Levy, Free energy surfaces of beta-hairpin and alpha-helical peptides generated by replica exchange molecular dynamics with the AGBNP implicit solvent model, Proteins 56 (2004) 310–321.
[35] E.J. Sorin, Y.M. Rhee, B.J. Nakatani, V.S. Pande, Insights into nucleic acid conformational dynamics from massively parallel stochastic simulations, Biophysical Journal 85 (2003) 790–803.
[36] V. Hornak, R. Abel, A. Okur, B. Strockbine, A. Roitberg, C. Simmerling, Comparison of multiple amber force fields and development of improved protein backbone parameters, Proteins 65 (2006) 712–725.
[37] R.B. Best, N.V. Buchete, G. Hummer, Are current molecular dynamics force fields too helical? Biophysical Journal 95 (2008) L7–L9.
[38] W. Humphrey, A. Dalke, K. Schulten, VMD: Visual molecular dynamics, Journal of Molecular Graphics 14 (1996) 33–38.
[39] M. Heinig, D. Frishman, STRIDE: a web server for secondary structure assignment from known atomic coordinates of proteins, Nucleic Acids Research 32 (2004) W500–W502.
[40] E. Rosta, H.L. Woodcock, B.R. Brooks, G. Hummer, Artificial reaction coordinate "tunneling" in free-energy calculations: the catalytic reaction of RNase H, Journal of Computational Chemistry 30 (2009) 1634–1641.
[41] M. Seeber, M. Cecchini, F. Rao, G. Settanni, A. Caflisch, Wordom: a program for efficient analysis of molecular dynamics simulations, Bioinformatics 23 (2007) 2625–2627.
[42] F. Noe, C. Schutte, E. Vanden-Eijnden, L. Reich, T.R. Weikl, Constructing the equilibrium ensemble of folding pathways from short off-equilibrium simulations, Proceedings of the National Academy of Sciences of the United States of America 106 (2009) 19011–19016.
[43] A. Jain, R. Hegger, G. Stock, Hidden Complexity of Protein Free-Energy Landscapes Revealed by Principal Component Analysis by Parts, Journal of Physical Chemistry Letters 1 (2010) 2769–2773.
[44] A.E. Garcia, Large-Amplitude Nonlinear Motions in Proteins, Physical Review Letters 68 (1992) 2696–2699.
[45] A. Rajan, P.L. Freddolino, K. Schulten, Going beyond Clustering in MD Trajectory Analysis: An Application to Villin Headpiece Folding, PLoS One 5 (2010) 12.
[46] R.A. Jarvis, E.A. Patrick, Clustering Using a Similarity Measure Based on Shared near Neighbors, IEEE Transactions on Computers C-22 (1973) 1025–1034.